www.czasopisma.pan.pl PAN POLSKA AKADEMIA NAUK www.journals.pan.pl

Arch. Metall. Mater. **65** (2020), 2, 601-608

DOI: 10.24425/amm.2020.132798

E. RUDNIK[1*]

RECOVERY OF ZINC FROM STEELMAKING FLUE DUST BY HYDROMETALLURGICAL ROUTE

Industrial steelmaking (EAF) flue dust was characterized in terms of chemical and phase compositions, leaching behaviour in 20% sulphuric acid solution as well as leaching thermal effect. Waste product contained about 43% Zn, 27% Fe, 19% O, about 3% Pb and Mn and lesser amounts of other elements (Ca, Si, Mo, etc.). It consisted mainly of oxide-type compounds of iron and zinc. Dissolution of metals (Zn, Fe, Mn) from the dust was determined in a dependence of solid to liquid ratio (50-200 g/L), temperature (20-80ºC) and leaching time (up to 120 min). The best result of 60% zinc recovery was obtained for 50 g dust/L and a temperature of 80ºC. Leaching of the material was an exothermic process with a reaction heat of about –318 kJ/kg. Precipitation purification of the solution was realized using various ratios of H_2O_2 to NH_{3aq}. A product of this stage was hydrated iron(III) oxide. Final solution was used for zinc electrowinning. Despite that pure zinc was obtained the highest cathodic current efficiency was only 40%.

Keywords: EAF dust; leaching; electrowinning; recycling

1. Introduction

Today, recycling of non-ferrous metals is of great significance to preserve natural resources and protect environment. Zinc is the fourth of the most important technical metals after iron, aluminum and copper. More than half of annual production of metallic zinc is used to protect iron and steel against corrosion [1]. After their lifetime, galvanized steel products, like car bodies or construction elements, are recycled by steel mills. It is estimated that about 55% of steel produced in Europe originates from the recycling of the steel scrap. It corresponded to 93.35 million tonnes of steel scraps consumed in 2017 in the European Union (28) [2]. About 40% of the European crude steel production is realized by electric arc furnace (EAF) procedure. The off gases of the EAF process are cleaned and 15-23 kg of filter dust are collected per one tonne of steel produced [3]. It translates to 1-1.5 million tonnes of the EAF dust being generated annually (EU-28). The EAF dust represents hazardous waste and is collected under European Waste Catalogue number of 10 02 07* [4]. Its disposal is costly and requires special secure landfills due to a possible elution of heavy metals and, thus, pollution of the environment [5, 6]. Otherwise, utilization of the EAF dusts for production of ceramics, concrete, cement clinker, industrial glass [7-9] has gained attention recently.

The EAF dusts consist mainly of iron oxides, but they contain also zinc due to its high volatility and accumulation in the dust during thermal treatment of the galvanized steel scraps. Concentration of zinc in the EAF dusts ranges from 4 wt% to 45 wt%, depending on the scrap's source region, composition of the batch, heat treatment conditions, etc. [3, 10-21]. About 70% of the EAF dust generated in Europe is currently recycled in a Waelz kiln process. However, there are some disadvantages of such treatment like: zinc and lead remain in the slag where iron is not sufficiently enriched after vaporization separation of zinc, zinc content in the dust must be higher than 16 wt% to guarantee economics of the process and, finally, high energy consumption due to strict temperature requirements [21]. Alternatively to the pyrometallurgical treatment, hydrometallurgical methods for zinc recovery from the EAF dusts were proposed. It was reported that sulphuric, hydrochloric, nitric and citric acid solutions [11-16] can be more or less effective for the leaching of the EAF dusts, while sodium hydroxide is selective for zinc dissolution from the waste [17-20]. Non-conventional aqueous (hydrogen nitrilotriacetate) [22] or non-aqueous (choline chloride-urea ionic liquid) [23] leachants for the zinc recovery were also investigated. Further solution purification and final recovery of zinc is dependent on the leaching stage. Thus, hematite [13], goethite [24], jarosite [25] or zinc basic carbonate [26] precipitation from

[1] AGH UNIVERSITY OF SCIENCE AND TECHNOLOGY, FACULTY OF NON-FERROUS METALS, AL. MICKIEWICZA 30, 30-059 KRAKÓW, POLAND

* Corresponding author: erudnik@agh.edu.pl

acid solutions was proposed. In turn, lead cementation with zinc powder followed by zinc electrowinning from alkaline solutions was reported [18,20].

The present paper shows results of acidic leaching of steelmaking flue dust. The influence of temperature, solid phase content in sulphuric acid solution and leaching time on the transfer of main leachable dust's components (Fe, Zn, Mn) to the liquid phase was determined. The leaching stage was followed by iron(III) precipitation using concentrated ammonia under oxidative conditions and zinc electrowinning.

2. Experimental

Steelmaking flue dust used in this study originated from industrial recycling of steel scraps by EAF process. Morphology of the material was examined with a scanning electron microscope (SEM, Hitachi). Specimen was prepared by mounting the powder in a conductive carbon resin. General and detailed analysis of the elemental composition of the waste was performed using energy dispersive X-ray spectroscopy (EDS) method. Phase composition of the material was identified by X-ray diffractometry.

The material was treated as received from the plant. It was leached in one stage (120 min) using 20% H_2SO_4 at various temperatures (20-80°C). The acid concentration was selected according to theoretical calculations upon metal percentages in the initial material and the dust amounts used in the leaching experiments. 200 cm^3 of the acid and 50-200 g/L of the solids (i.e. liquid to solid ratios in a range of 20-5) were used. The suspensions were stirred with a magnetic stirrer at an agitation rate of 400 rpm. During the process, samples of the electrolyte were taken periodically to determine concentration of metal ions. pH of the solutions (Crison pH-meter) and concentration of the acid (titration with 0.1 M NaOH in the presence of methyl orange as an indicator) were determined before and after the process. After completed leaching, solid residues were collected, washed, dried and weighed.

Efficiency of zinc leaching η (in %) was calculated according to the formula:

$$\eta = \frac{c \cdot V}{P_{Zn} \cdot m} \cdot 10^4 = \frac{c}{P_{Zn} \cdot L} \cdot 10^4 \qquad (1)$$

where: c – final concentration of Zn(II) ions in the solution in g/L, V – volume of leachate in L, m – mass of EAF dust used in the leaching in g, P_{Zn} – average percentage of zinc in the dust, L – content of the dust in the solution in g/L.

Thermal effect of the leaching was determined using calorimetric method. Measurements were performed using isolated glass container equipped with a magnetic stirrer (400 rpm). 150 g/L of the dust was added to 100 cm^3 of 20% H_2SO_4 of known initial temperature. The temperature of the leaching system was monitored every 15 s. The temperature difference before and completed process was determined graphically to evaluate the heat released during the reaction.

Precipitation purification of the selected leaching solutions was carried out by adding 25% ammonia solution under oxidizing conditions (30% H_2O_2) at a temperature of 50°C (400 rpm). Three options were examined, i.e. by using twofold excess and/or not of $NH_{3\ aq}$ and H_2O_2. The amounts of the reagents were calculated in the relation to the amount of iron and zinc ions in the solution (more explanation is shown in a paragraph 3.3).

Zinc electrowinning was carried out from the solutions obtained after purification stage. They contained 20-25 g Zn(II)/L. Before electrolysis the solutions were acidified with H_2SO_4 to pH of 1.0 ± 0.1. The electrolysis was carried out for 30 min, at cathodic current densities of 2-4 A/dm^2 and at ambient temperature (20°C). An aluminum plate as a cathode substrate and two lead plates as anodes were used. The solution was agitated with a magnetic stirrer (200 rpm).

At all stages of the experiments, concentrations of the metal ions were determined using atomic absorption spectrometry (Solaar M5, ThermoElemental), while solid products were analyzed by means of X-ray diffractometer (Rigaku MiniFlex diffractometer, $Cu_{K\alpha}$ radiation).

3. Results and discussion

3.1. Characterization of EAF dust

The flue dust from industrial EAF installation was dark brown powdery mixture of magnetic and nonmagnetic compounds (Fig. 1a). EDS analysis carried out on sixteen areas (e.g. Fig. 1b) of the sample surface indicated about 43% Zn, 27% Fe, 19% O, 3% Pb and Mn, as well as other elements like Si, Mo, Ca, etc. (Tab. 1). The dust characterized with low concentration of chlorine and fluorine (each about 0.5%). More detailed analysis of the results showed quite good homogeneity of the waste. It consisted of the particles of relatively stable zinc, iron and manganese contents, but variable proportions of oxygen (9-25%) and lead (0-5.7%).

TABLE 1

Average composition of EAF dust

Element	Composition, wt%
Zn	42.68 ± 4.50
Fe	26.95 ± 2.43
Pb	3.20 ± 1.43
Mn	2.97 ± 0.22
Si	1.67 ± 0.42
Mo	1.50 ± 0.47
Ca	1.29 ± 0.49
Al	0.67 ± 0.23
Cr	0.40 ± 0.05
Mg	0.37 ± 0.11
K	0.30 ± 0.07
O	19.18 ± 4.96
S	0.86 ± 0.76
Cl	0.52 ± 0.22
F	0.40 ± 0.23
P	0.13 ± 0.03

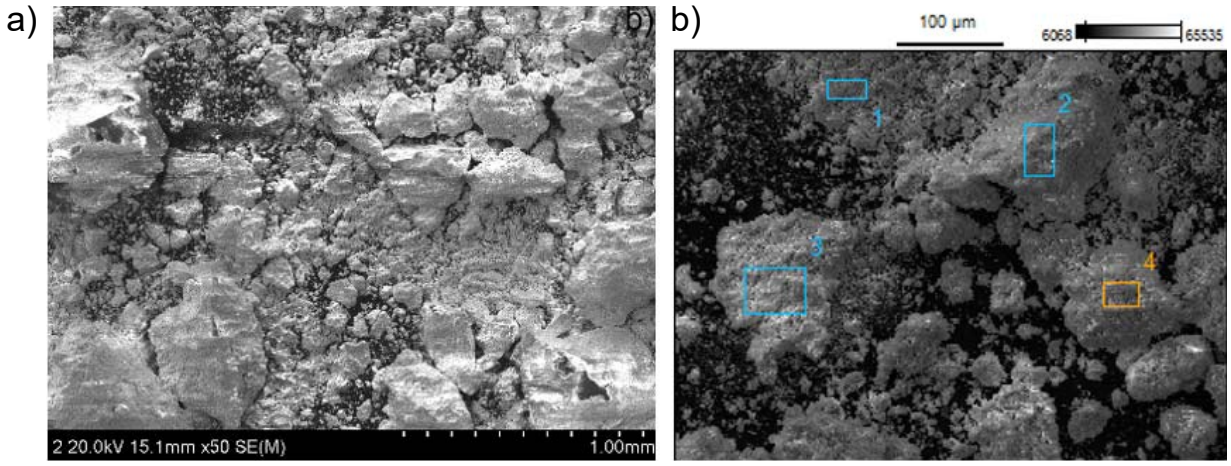

Fig. 1. Morphology of EAF dust: a) general view, b) areas of local elemental analysis

Phase analysis (Fig. 2) indicated main compounds in the dust. These were iron oxides (Fe_2O_3, Fe_3O_4), zincite (ZnO) and franklinite ($ZnFe_2O_4$). The presence of iron manganese oxide ($FeMnO_3$) was not excluded. Lead oxides were not identified due to detection limits for crystalline components of low concentrations.

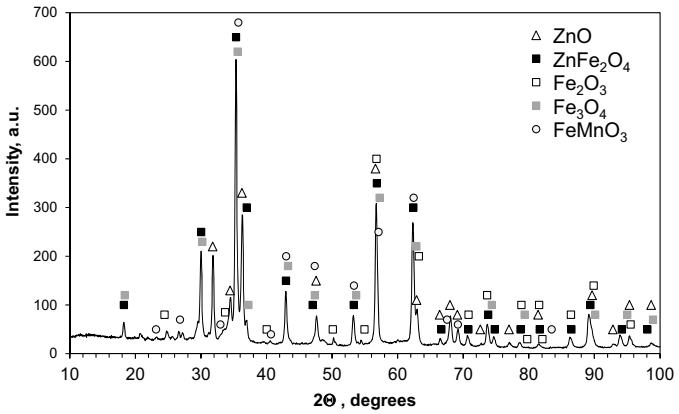

Fig. 2. XRD pattern of EAF dust

Comparison of the results with other reports shows that general phase composition of the EAF dusts is independent of world's region, thus zinc and iron oxides as well as franklinite are always present [7-24]. The main differences are related to the proportions of the particular elements. However, it should be emphasised that actual composition of the EAF dusts may be quite complicated. For example, Sofilić et al. [10] identified over fifty chemical compounds in twelve dust samples taken monthly for one year from the same steel mill. The samples characterized with similar percentages of the metals (e.g. 44 ± 4% Fe, 6 ± 2% Zn, 5.5 ± 0.3% Mn), but changeable phase composition. Hence, various oxides, mixed oxides, sulphides and/or sulphates of iron, zinc, manganese, aluminum, silicon, copper, nickel, lead, calcium, etc. were found in the EAF dusts.

3.2. Leaching of dust

The dust samples were leached in 20% H_2SO_4 at various temperatures. Figures 3-5 show changes of metal ions concentrations in the solutions during leaching different amounts of the material. In each case, concentration of zinc ions reached almost constant level during first hour of the process (Fig. 3), while prolongation of the process increased contamination of the solution by iron (Fig. 4) and manganese (Fig. 5). Growing amounts of the solid in the solution from 50 g/L to 200 g/L resulted in higher final concentrations of zinc ions from 10 g/L (20-40°C) and 20 g/L (60-80°C) to 35 g/L (20-60°C) and 45 g/L (80°C), respectively. However, after the leaching at the highest temperature, crystallization of salts in the solution was observed after filtration and cooling to the room temperature.

Iron and manganese were the main impurities of the solutions. The increase in the dust concentration from 50 g/L to 200 g/L corresponded to raising of Fe(II, III) ions concentrations from 2-4 g/L (20-40°C) and 5-6 g/L (60-80°C) to 8-13 g/L (20-40°C) and 18-22 g/L (60-80°C), respectively. In turn, Mn(II) ions concentrations were 0.5-1 g/L (20-80°C) for 50 g dust/L to 1.6-3.8 g/L (20-80°C) for 200 g dust/L.

Figure 6 summarizes efficiency of the zinc leaching. It was found that solubility of the dust and, thus, leachability of zinc decreased with increased content of the dust in the bath at the constant temperature. However, the increase in the temperature was advantageous for the zinc leaching giving the highest efficiencies in the range of 53-60% at 80°C.

Solid residues were collected after the completed leaching. They represented 66 ± 2% (20 and 40°C) or 39 ± 0.7% (60 and 80°C) of the initial sample mass. Phase analysis of the solid residues (not shown) indicated the presence of only one insoluble component $PbSO_4$ formed as a product of the reaction of lead oxide with sulphuric acid. The presence of lead oxides was expected according to the results of EDS analysis, but lead compounds were not detected in the diffraction pattern of the dust. More detailed analysis of the filtrate cake revealed a mixture of magnetic and non-magnetic fractions. Figure 7 shows examples of X-ray diffractograms of the individual fractions of the

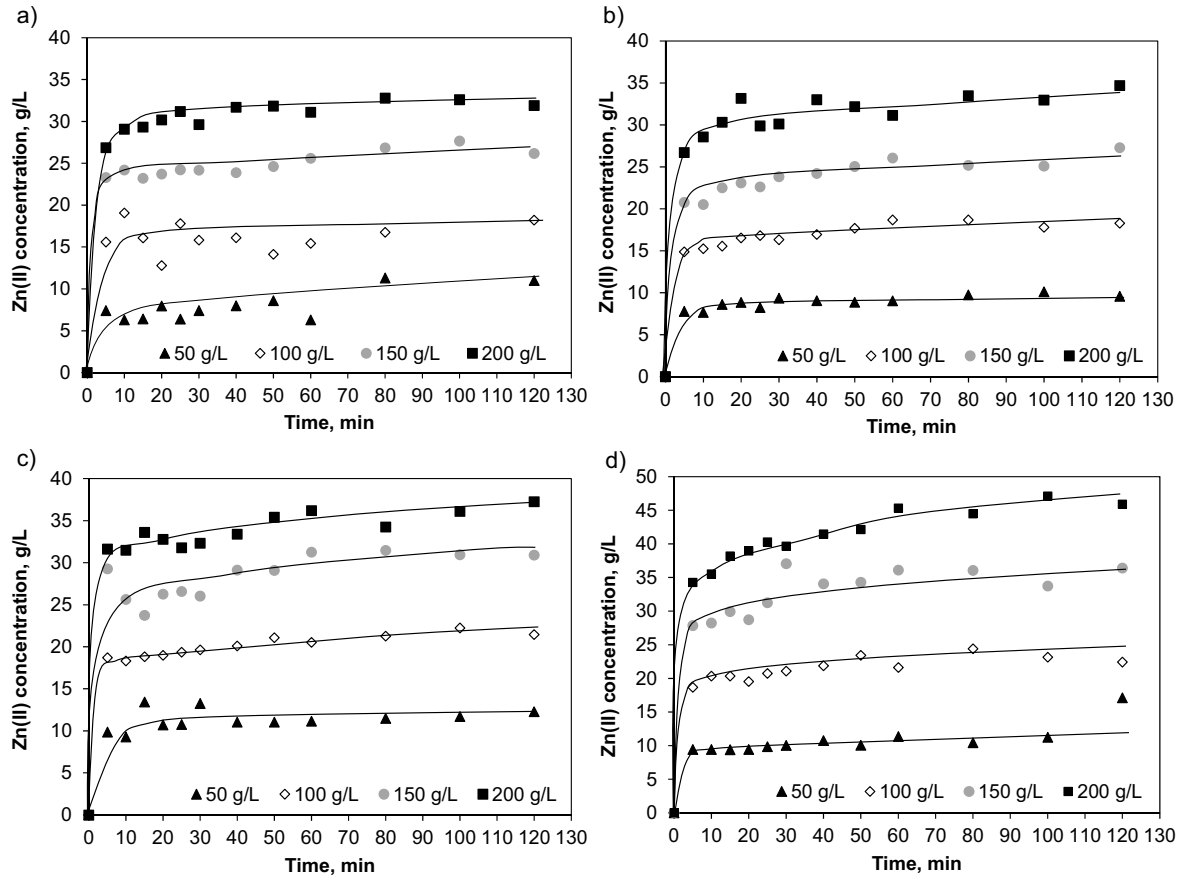

Fig. 3. Influence of leaching time and EAFD content on concentration of zinc ions in solution

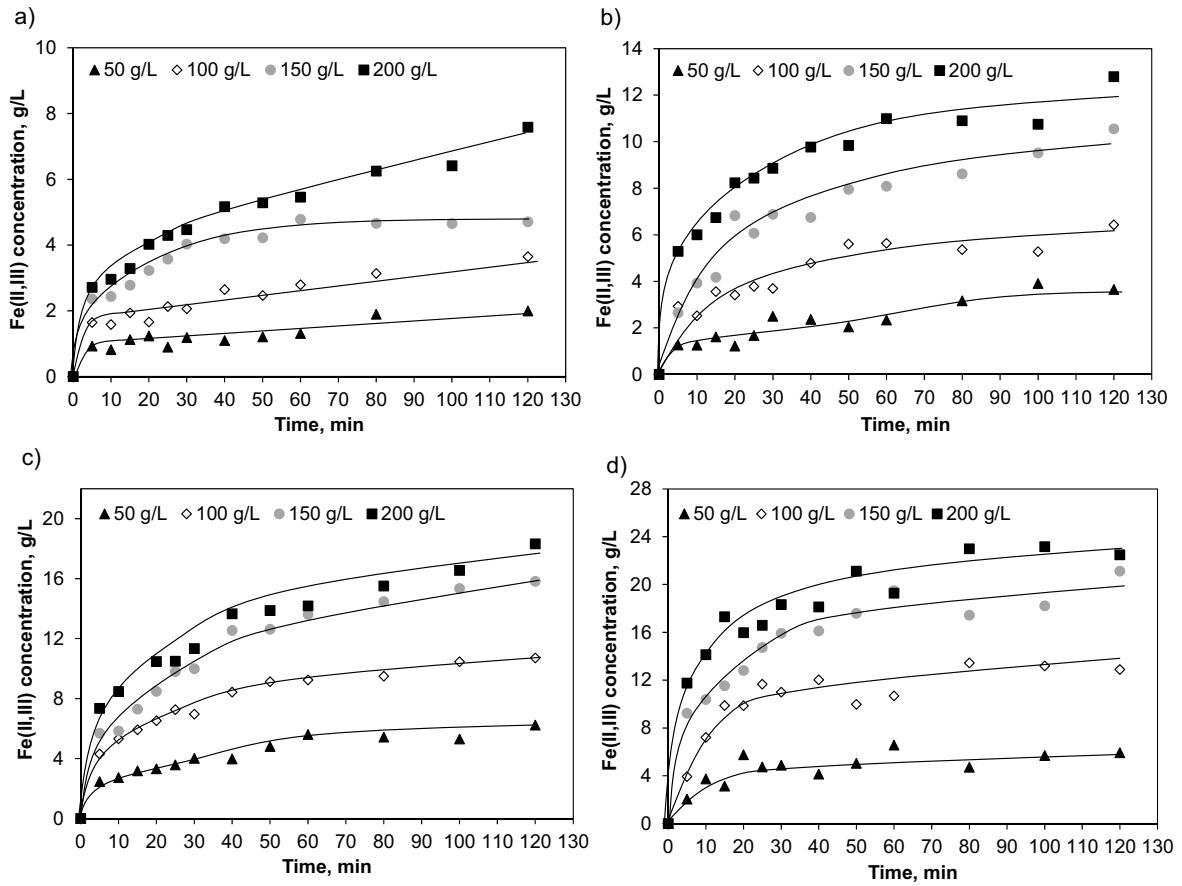

Fig. 4. Influence of leaching time and EAFD content on concentration of iron ions in solution

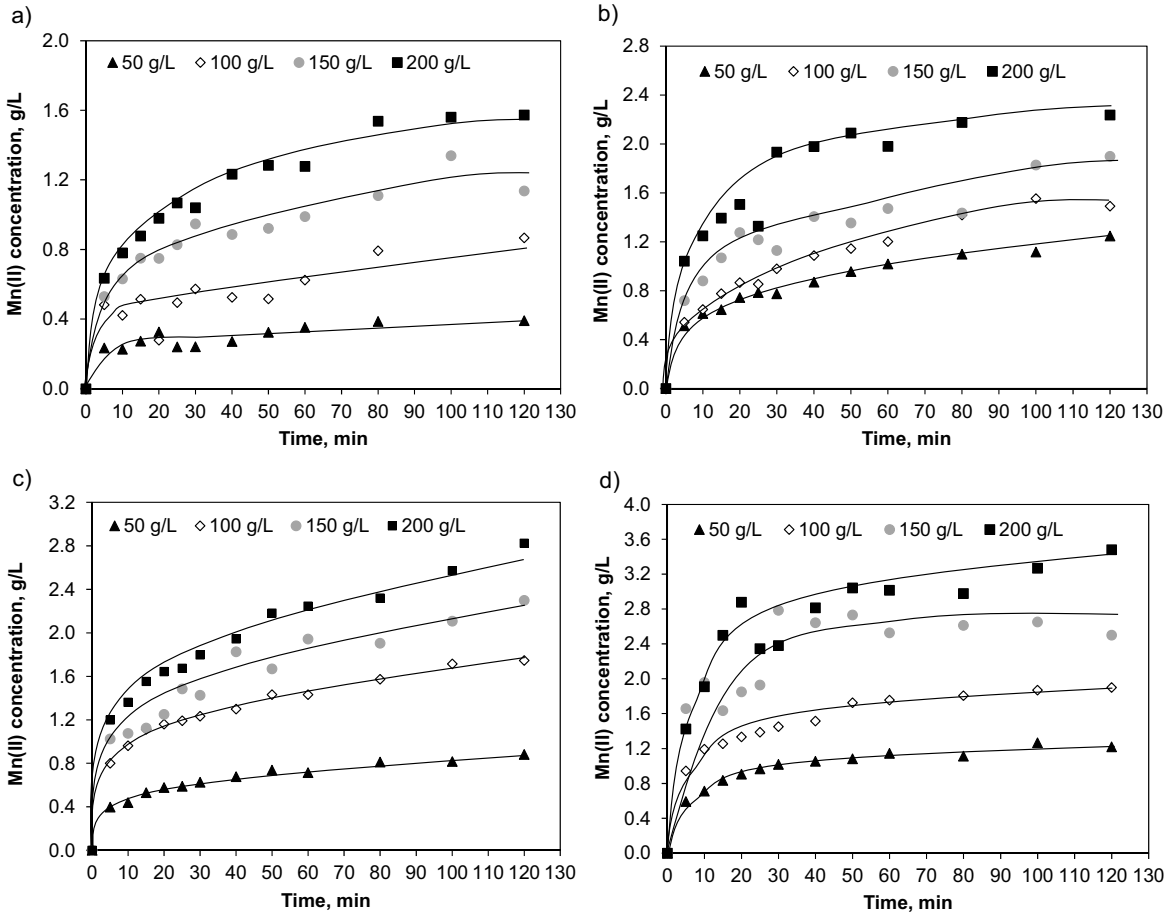

Fig. 5. Influence of leaching time and EAFD content on concentration of manganese ions in solution

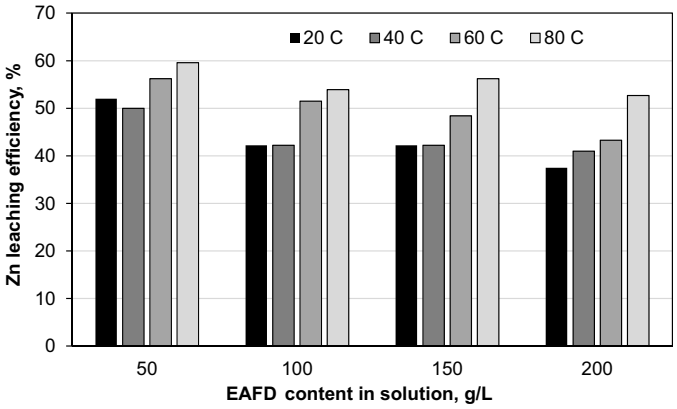

Fig. 6. Influence of leaching conditions on efficiency of zinc extraction

residue. They indicated the presence of refractory franklinite and mixed iron-zinc oxide being the reasons of incomplete dissolution of zinc despite of existence of free acid in the final leachate (Tab. 2). This is consistent with thermodynamic considerations (Tab. 3) showing a reaction of franklinite with sulphuric acid as less preferable, but possible, due to less negative change of standard free energy of the reaction ΔG_r^o in a comparison to the ΔG_r^o value for the reaction of the acid with zinc oxide. However, it must be emphasized that thermodynamic deliberations are not solely factors determining a course of the reactions and other factors like kinetics can govern the particular processes.

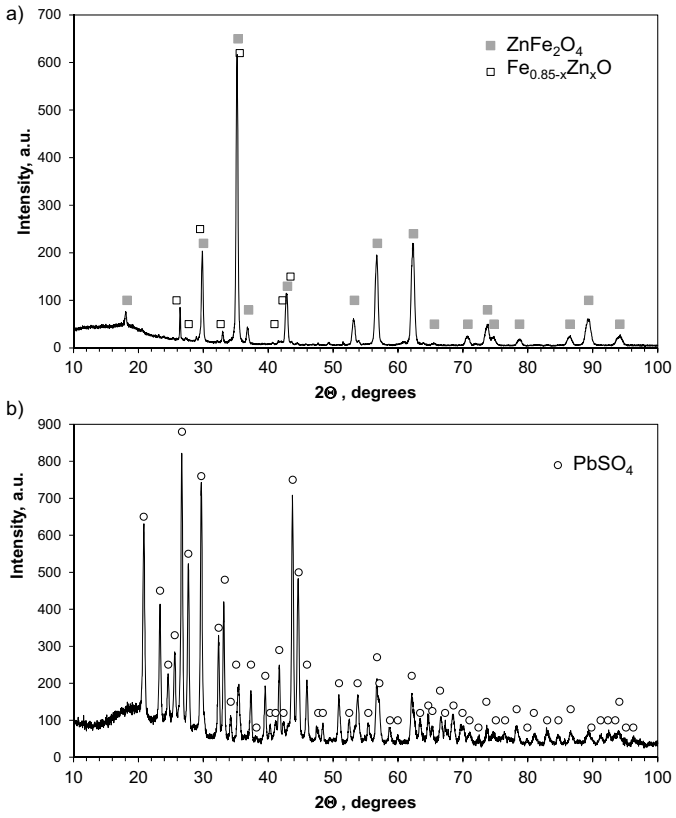

Fig. 7. XRD pattern of solid residues after leaching (50 g/L, 80°C): a) magnetic fraction, b) nonmagnetic fraction

TABLE 2

H_2SO_4 concentrations in solutions after leaching. Initial H_2SO_4 concentration: 211 g/dm^3

Leaching conditions		After leaching	
EAFD content, g/L	**Temperature, °C**	**pH**	**H_2SO_4 concentration, g/dm^3**
50	20	–0.98	152.9 ± 1.0
100		–0.89	116.1 ± 0.0
150		–0.87	113.7 ± 0.5
200		–1.01	81.3 ± 0.0
50	40	–1.28	169.5 ± 6.9
100		–1.08	143.1 ± 1.0
150		–1.02	100.9 ± 0.0
200		–0.63	68.6 ± 0.0
50	60	–1.54	179.3 ±1.0
100		–1.32	137.2 ± 0.0
150		–1.24	84.8 ± 0.5
200		–0.69	61.3 ± 0.5
50	80	–1.16	171.0 ± 4.4
100		–1.16	114.7 ± 1.0
150		–0.90	76.4 ± 2.0
200		–0.41	42.1 ± 2.0

TABLE 3

Thermodynamic calculations related to EAF dust leaching in H_2SO_4. Basic thermodynamic data for 298.15 K taken from [27]

Reaction	ΔG_r^o, kJ	ΔH_r^o, kJ
$ZnO + 2H^+ \rightarrow Zn^{2+} + H_2O$	–64.0	–88.7
$ZnFe_2O_4 + 8H^+ \rightarrow Zn^{2+} + 2Fe^{3+} + 4H_2O$	–47.0	–208.3
$ZnFe_2O_4 + 2H^+ \rightarrow Zn^{2+} + 2FeO(OH)$	–48.8	–90.5
$ZnFe_2O_4 + 2H^+ + 2H_2O \rightarrow Zn^{2+} + 2Fe(OH)_3$	15.8	–39.7
$Fe_2O_3 + 6H^+ \rightarrow 2Fe^{3+} + 3H_2O$	–0.3	–131.0
$Fe_3O_4 + 8H^+ \rightarrow Fe^{2+} + 2Fe^{3+} + 4H_2O$	–59.1	–218.4

Increased dust content in the solution resulted in the higher final concentrations of the metal ions (Figs. 3-5) and lower free acid concentration and thus higher final pH at the constant temperature (Tab. 2). This is obvious due to consumption of the acid during leaching. However, at different temperatures (20-60 °C) but constant dust concentrations (50-100 g/L), an opposite tendency was found. In such cases, the concentration of free acid increased despite of higher final amounts of metal ion in the leachate. This effect was caused mainly by hydrolysis of soluble salts produced during leaching, mainly:

$$Fe_2(SO_4)_3 + (3+x)H_2O \rightarrow Fe_2O_3 \cdot xH_2O\downarrow + 3H_2SO_4 \quad (1)$$

Thermal effect of the leaching Q was determined from calorimetric measurement. During the leaching of the dust portion in H_2SO_4, a temperature was registered and plotted in Figure 8. It was observed that the reaction was rather fast and was accompanied by a rise of the temperature to a constant level. The temperature increase ΔT was determined graphically and used for the calculations according to the following formula:

$$Q = -\frac{\left(m_G \cdot c_G + m_A \cdot c_A\right) \cdot \Delta T}{m} \quad (2)$$

where: m_G – mass of the isolated glass reactor, m_A – mass of the acid solution, m – mass of the leached material, c_G – specific heat of glass (0.75 kJ/kg K), c_A – specific heat of 20% H_2SO_4 (3.53 kJ/kg·K) [28].

The temperature increase during the process was rather low (by about 10°C). The amount of the heat produced during the leaching was determined per 1 kg of the solid phase used and the value of –318 kJ/kg was obtained. It shows that the dissolution of the material is accompanied by the heat release. The experimental results can be confirmed by thermodynamic calculations, assuming that changes of standard reaction enthalpy ΔH_r^o can correspond to heat effects. The obtained results are summarized in Table 3. Negative values of ΔH_r^o represent exothermic character of the reactions, hence increased temperature may not result in a positive way on the course of the processes from thermodynamics point of view, but it can enhance kinetics of the reaction.

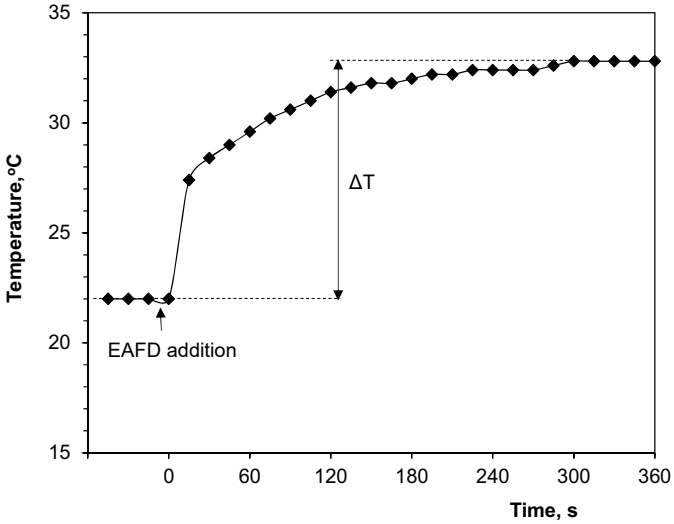

Fig. 8. Changes of temperature during calorimetric experiment (150 g EAFD/L)

Comparison of the data obtained in this study with results of acid leaching of the EAF dust shown by others authors showed that efficiency of the zinc dissolution under atmospheric pressure is dependent on a few factors. These are: percentage of zinc as oxide in the dust, H_2SO_4 concentration, liquid to solid ratio (L/S) and temperature. For example, Langová et al. [24] reported almost 100% zinc extraction in 3M H_2SO_4 at 80°C and L/S ratio of 5 (6 h of leaching), but the EAF dust contained only 8% Zn (at 45% Fe). It was also shown [12,29] that high zinc recovery of 70-80% can be obtained in 1M H_2SO_4 for high L/S ratios of 12.5 (33% Zn, 26% Fe in the dust) or 50 (17% Zn, 27% Fe in the dust) at the same temperature. A good selectivity with regard to zinc altogether with the high zinc extraction (70%) was achieved in 0.4-0.5 M H_2SO_4 at 80°C and L/S of 30 or 50 [12,30]. Shawabkeh [15] obtained about 70% zinc extraction from the dust (29% Zn, 24% Fe) even in 0.1 M H_2SO_4 at 50°C, but the dust concentration in the solution was only 1-3 g/L, whereas a half of total zinc existed as ZnO.

3.3. Solution purification

Removal of iron ions from the solutions of relatively high concentrations of Fe(II, III) (10-20 g/L) and Zn(II) (20-40 g/L) is very arduous and ineffective if traditional calcium carbonate is used for solution alkalization and iron precipitation. Therefore, ammonium was selected as iron(III) precipitant and zinc(II) complexing agent:

$$Fe^{3+} + 3NH_3 \cdot H_2O \rightarrow Fe(OH)_3 \downarrow + 3NH_4^+ \quad (3)$$

$$Zn^{2+} + 4NH_3 \rightarrow Zn(NH_3)_4^{2+} \quad (4)$$

Three tests were performed: (i) both H_2O_2 and NH_{3aq} in excess, (ii) stoichiometric amount of H_2O_2 and NH_{3aq} in excess, (iii) stoichiometric amounts of both H_2O_2 and NH_{3aq}. Stoichiometric amount of hydrogen peroxide was calculated according to the content of iron ions in the solution. It was added to oxidize Fe(II) to Fe(III) ions:

$$2Fe^{2+} + H_2O_2 + 2H^+ \rightarrow 2Fe^{3+} + 2H_2O \quad (5)$$

In turn, stoichiometric amount of ammonia was calculated according to the equations (3)-(4) and corresponding metal ions concentrations. Addition of ammonia resulted in the final pH of the suspensions (and also filtrates) in a range of 6.2-6.9, independently on the amount added. It seems that rather relatively high temperature of the precipitation (50°C) could enhance evaporation of ammonia from the reaction system.

Final precipitate was filtered and washed with diluted ammonia solution to remove zinc from the residue . If it was done incorrectly, basic zinc sulphates were detected in the dried solid (Fig. 9). Pure residue consisted of hydrated iron(III) oxide $Fe_2O_3 \cdot H_2O$ correlated with goethite in a nature according to one of the XRD standards (No. 00-002-0281).

3.4. Zinc electrowinning

Electrowinning of zinc was carried out from purified solutions containing 20-25 g Zn(II)/L and below: 0.2 g/L Mn(II) and 0.01 g/L Fe(III). Table 4 summarizes results of the electrolysis.

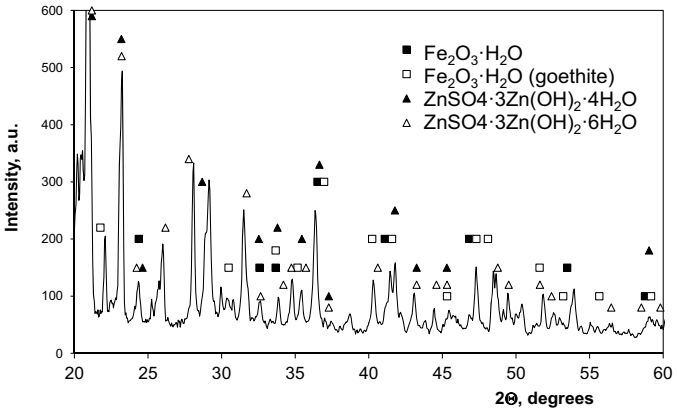

Fig. 9. XRD pattern of unwashed well solid product of precipitation purification

Direct relationships between purification procedure and efficiency of the cathodic process were found. Low cathodic current efficiencies were obtained if excess of ammonia was used. It was caused by side cathodic reactions taking place on the cathode:

$$2H^+ + 2e \rightarrow H_2 \quad (6)$$

$$2NH_4^+ + 2e \rightarrow H_2 + 2NH_3 \quad (7)$$

There is a little information in the literature about cathodic reduction of ammonium cation [31,32], but the simplest electrode reaction (7) has been assumed. The calculated standard potential for such reaction is –0.651 V [31] indicating favouritism of the reaction in comparison to the zinc ion reduction.

Electrolysis voltage was in a range of 3.2-3.6 V, typical for zinc electrowinning. Voltage only slightly increased with the current density, however, at low current efficiencies it resulted in high energy consumption.

The presence of NH_4^+ and H_2O_2 residues in the electrolyte changed appearance of zinc deposits. Powdery black deposits were obtained for (i) purification variant, while for remaining solutions dark gray or gray, compact, fine-grained deposits were formed. In all cases, phase analysis confirmed metallic zinc product. XRF analysis detected pure zinc (the presence of metallic impurities was questionable due to quantitative limitations of the method used).

TABLE 4

Current efficiency and energy consumption during zinc electrowinning (pH 1.0 ± 0.1)

Precipitation purification conditions	Cathodic current density, A/dm^2	Cathodic current efficiency, %	Electrolysis voltage, V	Energy consumption, kWh/kg	Zinc deposit
H_2O_2 excess NH_{3aq} excess	2 3 4	25.5 18.2 34.3	3.2 3.2 3.6	13.3 18.7 11.1	black, powdery
H_2O_2 stoichiometric NH_{3aq} excess	2 3 3 4	9.0 15.2 16.6 14.9	3.1 3.2 3.4 3.4	36.6 22.3 21.8 24.2	dark gray, compact
H_2O_2 stoichiometric NH_{3aq} stoichiometric	2 3 4	38.4 40.3 41.0	3.4 3.6 3.8	9.4 9.5 9.8	gray, compact

The obtained results shows that the optimal electrolysis conditions corresponding to about 40% cathodic current efficiency were for the electrolytes with no excess reagents used in the purification stage.

4. Conclusions

The EAF dust with a total zinc content of approx. 43% contained mainly oxide compounds of zinc and iron, with small fractions of lead and manganese. The material was relatively hard-leachable in sulphuric acid, even at elevated temperature (80°C). Under these conditions, the final concentration of zinc ions reached a maximum of 45 g/L (200 g dust/L). The highest zinc extraction of 60% was for 50 g dust/L. Precipitation method (after Fe(II) oxidation with H_2O_2) was used for the leachate purification by gradual dosing of concentrated ammonia to a pH of about 6-7. Well washing of hydrated iron(III) precipitate prevents losses of zinc from the solution. The electrolytic zinc recovery was carried out in the current density range of 2-4 A/dm^2 without deterioration of the quality of the layers if no excess of reagents were used in the purification stage. The electrolysis voltage reached values typical for zinc electrowinning, but low current efficiency led to high energy consumption.

Finally, it should be noted that further improvement of zinc leaching from the EAF dust with sulphuric acid can be achieved by an application of ultrasounds [33] or microwaves [34].

Acknowledgments

This work was carried out in a cooperation with OKSYMET Sp. z.o.o. (Skawina, Poland).

REFERENCES

[1] www.zinc.org, accessed: 17.02.2019.
[2] World steel recycling in figures 2013-2017, Bureau of International Recycling, Ferrous Division, Brussels (2018).
[3] J. Antrekowitsch, S. Steinlechner, A. Unger, G. Rösler, R. Pichler, R. Rumpold, Zinc and Residue Recycling, in: Handbook of recycling, Elsevier, 113-124 (2014).
[4] 2014/955/EU: Commission Decision of 18 December 2014 amending Decision 2000/532/EC on the list of waste pursuant to Directive 2008/98/EC of the European Parliament and of the Council (2014).
[5] M.G. Sebag, C. Korzenowski, A.M. Bernardes, A.C. Vilela, J. Hazard. Mater. **166**, 670-675 (2009).
[6] T.A. Lytaeva, A.E. Isakov, J. Ecol. Eng. **18** (3), 37-42 (2017).
[7] C. Sikalidis, M. Mitrakas, J. Environ. Sci. Health Part A: Toxic/Hazard Subst. Environ. Eng. **41** (9), 1943-1954 (2006).
[8] T. Lis, K. Nowacki, Steel Res. Int. **83** (9), 842-851 (2012).
[9] C.M.F. Vieira, R. Sanchez, S.N. Monteiro, N. Lalla, N. Quaranta, J. Mater. Res. Technol. **2** (2), 88-92 (2013).
[10] T. Sofilić, A. Rastovčan-Mioč, Š. Cerjan-Stefanović, V. Novosel-Radović, M. Jenko, J. Hazard. Mater. **B109**, 59-70 (2004).
[11] T. Havlik, B. Friedrich, S. Stopić, World Metall. Erzmetall. **57** (2), 113-120 (2004).
[12] F. Kukurugya, T. Vindt, T. Havlik, Hydrometall. **154**, 20-32 (2015).
[13] Š. Langová, D. Matýsek, Hydrometall. **101**, 171-173 (2010).
[14] P. Oustadakis, P.E. Tsakiridis, A. Katsiapi, S. Agatzini-Leonardou, J. Hazard. Mater. **179**, 1-7 (2010).
[15] R.A. Shawabkeh, Hydrometall. **104**, 61-65 (2010).
[16] P. Halli, J. Hamuyuni, H. Revitzer, M. Lundström, J. Clean. Prod. **164**, 265-276 (2017).
[17] A.J.B. Dutra, P.R.P. Paiva, L.M. Tavares, Min. Eng. **19**, 478-485 (2006).
[18] G. Orhan, Hydrometall. **78**, 236-245 (2005).
[19] A.A. Ghani, J. Saleem, Z.A. Hameed, H. Lal, M. Shoaib, Pak. J. Anal. Environ. Chem. **17** (1), 33-37 (2016).
[20] P. Palimąka, S. Pietrzyk, M. Stępień, K. Ciećko, I. Nejman, Metals, **8**, 547 (2018).
[21] X. Lin, Z. Peng, J. Yan, Z. Li, J-Y. Hwang, Y. Zhang, G. Li, T. Jiang, J. Clean. Prod. **149**, 1079-1100 (2017).
[22] A. Bakkar, J. Hazard. Mater. **280**, 191-199 (2014).
[23] N. Leclerc, E. Meux, J.-M. Lecuire, J. Hazard. Mater. **B91**, 257-270 (2002).
[24] Š. Langová, J. Riplová, S. Vallová, Hydrometall. **87**, 157-162 (2007).
[25] P.E. Tsakiridis, P. Oustadakis, A. Katsiapi, S. Agatzini-Leonardou, J. Hazard. Mater. **179**, 8-14 (2010).
[26] P. Xanthopoulos, S. Agatzini-Leonardou, P. Oustadakis, P.E. Tsakiridis, J. Environ. Chem. Eng. **5**, 3550-3559 (2017).
[27] R.A. Robie, B.S. Hemingway, Thermodynamic properties of minerals and related substances at 298.15K and 1 bar (10^5 Pascals) pressure and at higher temperatures. United States Government Printing Office, Washington (1995).
[28] J. Zienkowicz, I. Senderacka, W. Wallmoden (Eds.), Kalendarz chemiczny, PWT, Warszawa (in Polish) (1954).
[29] T. Havlik, B. Vidor e Souza, A.M. Bernardes, I.A.H. Schneider, A. Miskufova, J. Hazard. Mater. **B135**, 311-318 (2006).
[30] T. Havlik, M. Turzakova, S. Stopic, B. Friedrich, Hydrometall. **77**, 41-50 (2005).
[31] T. Bieszczad, S. Sanak-Rydlewska, Physicochem. Probl. Min. Process. **35**, 181-193 (2001).
[32] O. Berkh, Y. Shacham-Diamand, E. Gileadi, J. Electrochem. Soc. **155** (10), F223-F229 (2008).
[33] K. Brunelli, M. Dabalà, Int. J. Miner. Metall. Mater. **22**, 353-362 (2015).
[34] M. Al-Harahsheh, S.W. Kingman, Hydrometall. **73** (3-4), 189-203 (2004).